

# PEAK-TO-AVERAGE POWER RATIO OF SINGLE CARRIER FDMA SIGNALS WITH PULSE SHAPING

Hyung G. Myung                      Junsung Lim                      David J. Goodman  
 Department of Electrical and Computer Engineering, Polytechnic University  
 5 MetroTech Center, Brooklyn, NY 11201  
 USA  
 {hmyung01; jlim01} @utopia.poly.edu, dgoodman@poly.edu

## ABSTRACT

Single carrier frequency division multiple access (SC-FDMA), which utilizes single carrier modulation and frequency domain equalization is a technique that has similar performance and essentially the same overall complexity as those of OFDM, in which high peak-to-average power ratio (PAPR) is a major drawback. An outstanding advantage of SC-FDMA is its lower PAPR due to its single carrier structure. In this paper, we analyze the PAPR of SC-FDMA signals with pulse shaping. We analytically derive the time domain SC-FDMA signals and numerically compare PAPR characteristics using the complementary cumulative distribution function (CCDF) of PAPR. The results show that SC-FDMA signals indeed have lower PAPR compared to those of OFDMA. Comparing the two forms of SC-FDMA, we find that localized FDMA (LFDMA) has higher PAPR than interleaved FDMA (IFDMA) but somewhat lower PAPR than OFDMA. Also noticeable is the fact that pulse shaping increases PAPR.

## I. INTRODUCTION

Demands for media-rich wireless data services have brought much attention to high speed broadband mobile wireless techniques in recent years. Orthogonal frequency division multiplexing (OFDM), which is a multicarrier communication technique, has become widely accepted primarily because of its robustness against frequency selective fading channels which are common in broadband mobile wireless communications [1]. Orthogonal frequency division multiple access (OFDMA) is a multiple access scheme which is an extension of OFDM to accommodate multiple simultaneous users.

Despite the benefits of OFDM and OFDMA, they suffer a number of drawbacks including: high peak-to-average power ratio (PAPR); a need for an adaptive or coded scheme to overcome spectral nulls in the channel; and high sensitivity to frequency offset [2], [3].

Single carrier frequency division multiple access (SC-FDMA), which utilizes single carrier modulation and frequency domain equalization is a technique that has similar performance and essentially the same overall complexity as those of OFDMA system. One prominent advantage over OFDMA is that the SC-FDMA signal has lower PAPR because of its inherent single carrier structure [4]. SC-FDMA has drawn great attention as an attractive alternative to OFDMA, especially in the uplink communications where lower PAPR greatly benefits the mobile terminal in terms of

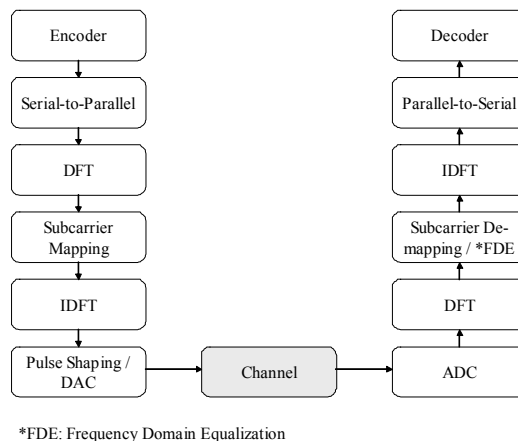


Fig. 1 Block diagram of SC-FDMA.

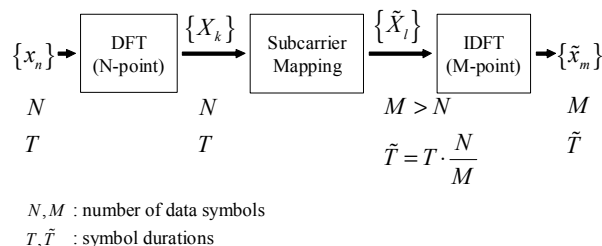


Fig. 2 Generation of SC-FDMA transmit symbols. There are  $M$  total number of carriers, among which  $N (< M)$  subcarriers are occupied by the input data.

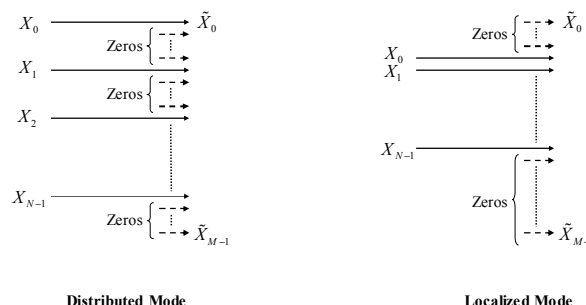


Fig. 3 Subcarrier mapping modes; distributed and localized modes.

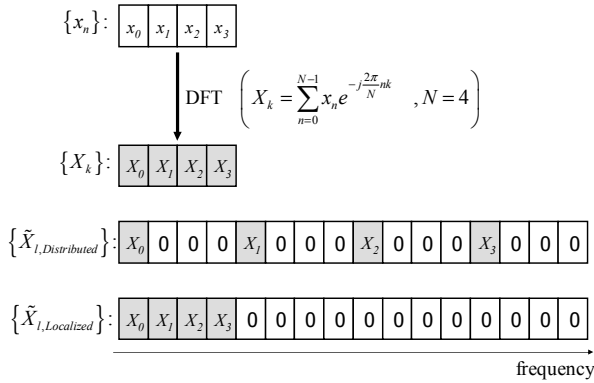


Fig. 4 An example of SC-FDMA transmit symbols in the frequency domain for  $N = 4$ ,  $Q = 4$  and  $M = 16$ .

$\tilde{X}_{l,Distributed}$  denotes transmit symbols for distributed subcarrier mapping mode and  $\tilde{X}_{l,Localized}$  denotes transmit symbols for localized subcarrier mapping mode.

transmit power efficiency. It is currently a strong candidate for uplink multiple access scheme in 3G Long Term Evolution of 3GPP [5].

In this paper, we analyze the PAPR of SC-FDMA signals and compare it with that of OFDMA. We analytically derive the time domain SC-FDMA signals and numerically compare PAPR characteristics using complementary cumulative distribution function (CCDF) of PAPR.

The remainder of this paper is organized as follows: Section II gives an overview of SC-FDMA. Section III derives the time domain signals for each subcarrier mapping mode of SC-FDMA and it presents the CCDF of PAPR obtained from Monte-Carlo simulations.

### II. OVERVIEW OF SC-FDMA SYSTEM

A block diagram of a SC-FDMA system is shown in Fig. 1. SC-FDMA can be regarded as discrete Fourier transform (DFT)-spread OFDMA, where time domain data symbols are transformed to frequency domain by DFT before going through OFDMA modulation. The orthogonality of the users stems from the fact that each user occupies different subcarriers in the frequency domain, similar to the case of OFDMA. Because the overall transmit signal is a single carrier signal, PAPR is inherently low compared to the case of OFDMA which produces a multicarrier signal.

Fig. 2 details the generation of SC-FDMA transmit symbols. There are  $M$  subcarriers, among which  $N (< M)$  subcarriers are occupied by the input data. In the time domain, the input data symbol has symbol duration of  $T$  seconds and the symbol duration is compressed to  $\tilde{T} = (N/M) \cdot T$  after going through SC-FDMA modulation.

There are two methods to choose the subcarriers for transmission as shown in Fig. 3. In the distributed subcarrier mapping mode, DFT outputs of the input data are allocated over the entire bandwidth with zeros occupying in unused subcarriers, whereas consecutive subcarriers are occupied by

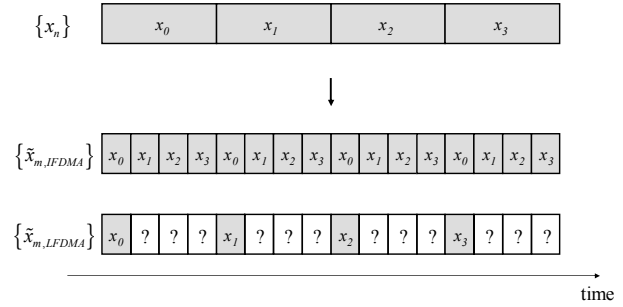


Fig. 5 An example of SC-FDMA transmit symbols in the time domain for  $N = 4$ ,  $Q = 4$  and  $M = 16$ .

the DFT outputs of the input data in the localized subcarrier mapping mode. We will refer to the localized subcarrier mapping mode of SC-FDMA as localized FDMA (LFDMA). The case of  $M = Q \cdot N$  for the distributed mode with equidistance between occupied subcarriers is called Interleaved FDMA (IFDMA) [6]. An example of SC-FDMA transmit symbols in the frequency domain for  $N = 4$ ,  $Q = 4$  and  $M = 16$  is illustrated in Fig. 4. After subcarrier mapping, the frequency data is transformed back to the time domain by applying inverse DFT (IDFT).

### III. PAPR OF SC-FDMA SIGNALS

In this section, we analyze the PAPR of the SC-FDMA signal for each subcarrier mapping mode. For distributed subcarrier mapping mode, we will consider the case of IFDMA. In the subsequent derivations, we will assume  $M = Q \cdot N$  and follow the notations in Fig. 2.

Let  $\{x_n : n = 0, 1, \dots, N-1\}$  be data symbols to be modulated. Then,  $\{X_k : k = 0, 1, \dots, N-1\}$  are frequency domain samples after DFT of  $\{x_n : n = 0, 1, \dots, N-1\}$ ,  $\{\tilde{X}_l : l = 0, 1, \dots, M-1\}$  are frequency domain samples after subcarrier mapping, and  $\{\tilde{x}_m : m = 0, 1, \dots, M-1\}$  are time symbols after IDFT of  $\{\tilde{X}_l : l = 0, 1, \dots, M-1\}$ . The complex passband transmit signal of SC-FDMA  $x(t)$  for a block of data is represented as

$$x(t) = e^{j\omega_c t} \sum_{m=0}^{M-1} \tilde{x}_m r(t - m\tilde{T}) \tag{1}$$

where  $\omega_c$  is the carrier frequency of the system and  $r(t)$  is the baseband pulse. In our research, we use a raised-cosine pulse, which is a widely used pulse shape in wireless communications, defined as follows in the time domain [7].

$$r(t) = \text{sinc}\left(\pi \frac{t}{\tilde{T}}\right) \frac{\cos\left(\frac{\pi\alpha t}{\tilde{T}}\right)}{1 - \frac{4\alpha^2 t^2}{\tilde{T}^2}} \tag{2}$$

where  $\alpha$  is the rolloff factor which ranges between 0 and 1. The PAPR is defined as follows for transmit signal  $x(t)$ .

$$\text{PAPR} = \frac{\text{peak power of } x(t)}{\text{average power of } x(t)} = \frac{\max_{0 \leq t \leq MT} |x(t)|^2}{\frac{1}{MT} \int_0^{MT} |x(t)|^2 dt} \quad (3)$$

Without pulse shaping, that is, using rectangular pulse shaping, symbol rate sampling will give the same PAPR as the continuous case since SC-FDMA signal is modulated over a single carrier. Thus, PAPR without pulse shaping with symbol rate sampling can be expressed as follows.

$$\text{PAPR} = \frac{\max_{m=0,1,\dots,M-1} |\tilde{x}_m|^2}{\frac{1}{M} \sum_{m=0}^{M-1} |\tilde{x}_m|^2} \quad (4)$$

We first examine the PAPR of transmit symbols for each block without pulse shaping analytically, and then, investigate the PAPR of transmit symbols with pulse shaping numerically.

#### A. Time domain symbols of IFDMA

For IFDMA, the frequency samples after subcarrier mapping  $\{\tilde{X}_l\}$  can be described as follows.

$$\tilde{X}_l = \begin{cases} X_{l/Q}, & l = Q \cdot k \quad (0 \leq k \leq N-1) \\ 0, & \text{otherwise} \end{cases} \quad (5)$$

We derive the time symbols  $\{\tilde{x}_m\}$  which are obtained by taking inverse DFT of  $\{\tilde{X}_l\}$ .

Let  $m = N \cdot q + n$ , where  $0 \leq q \leq Q-1$  and  $0 \leq n \leq N-1$ . Then,

$$\begin{aligned} \tilde{x}_m (= \tilde{x}_{Nq+n}) &= \frac{1}{M} \sum_{l=0}^{M-1} \tilde{X}_l e^{j2\pi \frac{ml}{M}} = \frac{1}{Q} \cdot \frac{1}{N} \sum_{k=0}^{N-1} X_k e^{j2\pi \frac{m}{N}k} \\ &= \frac{1}{Q} \cdot \frac{1}{N} \sum_{k=0}^{N-1} X_k e^{j2\pi \frac{Nq+n}{N}k} \\ &= \frac{1}{Q} \cdot \left( \frac{1}{N} \sum_{k=0}^{N-1} X_k e^{j2\pi \frac{n}{N}k} \right) \\ &= \frac{1}{Q} x_n \end{aligned} \quad (6)$$

The resulting time symbols  $\{\tilde{x}_m\}$  are simply a repetition of the original input symbols  $\{x_n\}$  in the time domain [6]. Therefore, the PAPR of IFDMA signal is the same as in the case of conventional single carrier signal. An example of an IFDMA signal is shown in Fig. 5.

#### B. Time domain symbols of LFDMA

For LFDMA, the frequency samples after subcarrier mapping  $\{\tilde{X}_l\}$  can be described as follows.

$$\tilde{X}_l = \begin{cases} X_l, & 0 \leq l \leq N-1 \\ 0, & N \leq l \leq M-1 \end{cases} \quad (7)$$

Let  $m = Q \cdot n + q$ , where  $0 \leq n \leq N-1$ , and  $0 \leq q \leq Q-1$ . Then,

$$\begin{aligned} \tilde{x}_m = \tilde{x}_{Qn+q} &= \frac{1}{M} \sum_{l=0}^{M-1} \tilde{X}_l e^{j2\pi \frac{ml}{M}} \\ &= \frac{1}{Q} \cdot \frac{1}{N} \sum_{l=0}^{N-1} X_l e^{j2\pi \frac{Qn+q}{QN}l} \end{aligned} \quad (8)$$

If  $q = 0$ , then,

$$\begin{aligned} \tilde{x}_m = \tilde{x}_{Qn} &= \frac{1}{Q} \cdot \frac{1}{N} \sum_{l=0}^{N-1} X_l e^{j2\pi \frac{Qn}{QN}l} \\ &= \frac{1}{Q} \cdot \frac{1}{N} \sum_{l=0}^{N-1} X_l e^{j2\pi \frac{n}{N}l} \\ &= \frac{1}{Q} x_n \end{aligned} \quad (9)$$

If  $q \neq 0$ , since  $X_l = \sum_{p=0}^{N-1} x_p e^{-j2\pi \frac{pl}{N}}$ , then (8) can be expressed as follows after derivation.

$$\tilde{x}_m = \tilde{x}_{Qn+q} = \frac{1}{Q} \left( 1 - e^{j2\pi \frac{q}{Q}} \right) \cdot \frac{1}{N} \sum_{p=0}^{N-1} \frac{x_p}{1 - e^{j2\pi \left\{ \frac{(n-p)q}{N} + \frac{q}{QN} \right\}}} \quad (10)$$

As can be seen from (9) and (10), in the time domain, LFDMA signal has exact copies of input time symbols in the  $N$ -multiple sample positions. In-between values are sum of all the time input symbols in the input block with different complex-weighting, which would increase the PAPR. An example of an LFDMA signal is shown in Fig. 5.

#### C. Numerical results

CCDF (Complementary Cumulative Distribution Function) of PAPR, which is the probability that PAPR is higher than a certain PAPR value  $\text{PAPR}_0$  ( $\Pr\{\text{PAPR} > \text{PAPR}_0\}$ ), is calculated by Monte Carlo simulation. CCDFs of PAPR for IFDMA, LFDMA, and OFDMA are evaluated and compared.  $10^5$  uniformly random data points were generated to acquire the CCDF of PAPR. Consecutive chunks were used for LFDMA, and in the case of OFDMA, transmission bandwidth of 5 MHz was assumed and 8 times oversampling was used when calculating PAPR [8]. No pulse shaping was applied in the case OFDMA. In the simulations, the total number of subcarriers  $M$  were set to 256, input data block size  $N$  to 64, and  $Q$  to 4. QPSK, 8-PSK, 16-QAM, 32-QAM, and 64-QAM

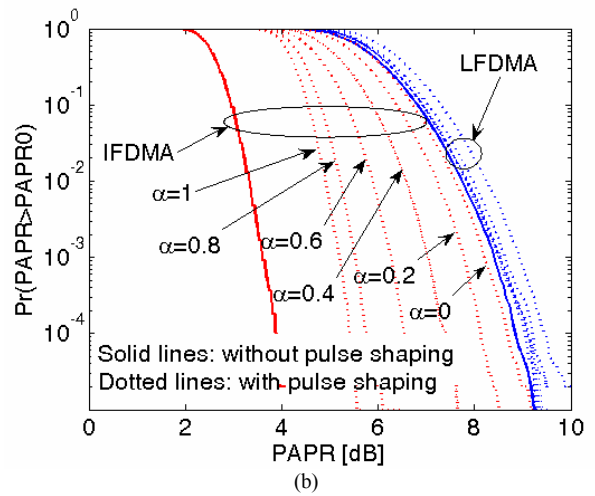
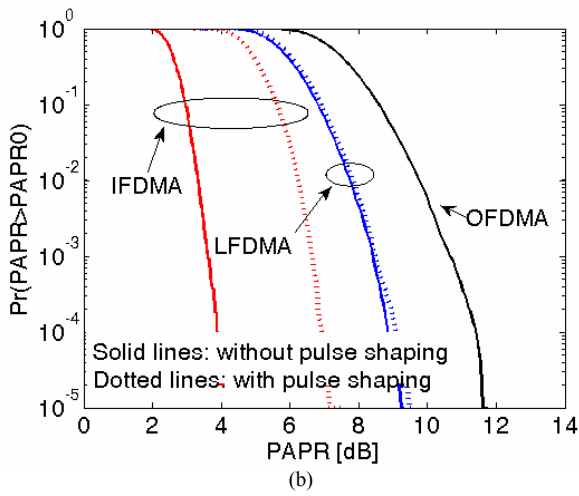
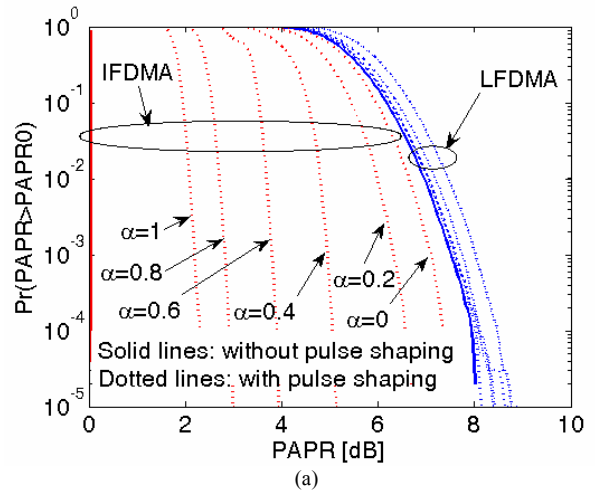
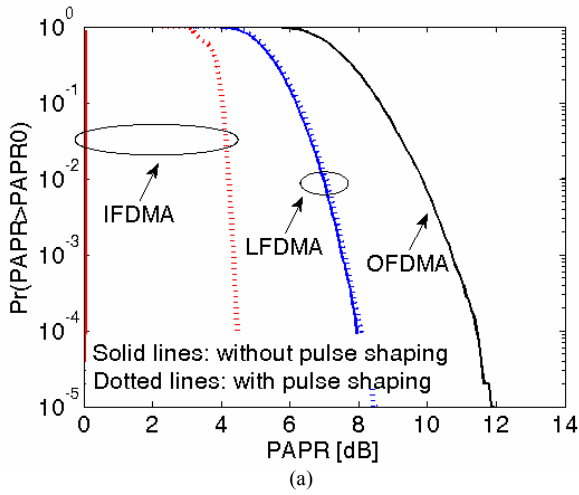


Fig. 6 Comparison of CCDF of PAPR for IFDMA, LFDMA, and OFDMA with  $M = 256$ ,  $N = 64$ , and  $\alpha = 0.5$ . (a) QPSK. (b) 16-QAM.

Fig. 7 Comparison of CCDF of PAPR for IFDMA and LFDMA with  $M = 256$ ,  $N = 64$ , and  $\alpha$  of 0, 0.2, 0.4, and 0.6, 0.8, and 1. (a) QPSK. (b) 16-QAM.

symbol constellations were considered. Raised cosine pulse  $r(t)$  was truncated from  $-6\tilde{T}$  to  $6\tilde{T}$  time period and it was oversampled by 8 times [7].

In Fig. 6, plots of CCDF of PAPR for IFDMA, LFDMA, and OFDMA are shown. We compare the PAPR value that is exceeded with probability less than 0.1% ( $\Pr\{PAPR > PAPR_0\} = 10^{-3}$ ), or 99.9-percentile PAPR. First, in the case of no pulse shaping, IFDMA has lower PAPR than the case of OFDMA by 10.5 dB for QPSK and by 7 dB for 16-QAM, while PAPR of LFDMA is lower than that of OFDMA by 3 dB for QPSK and by 2 dB for 16-QAM but higher than that of IFDMA by 7.5 for QPSK and by 5 dB for 16-QAM. With raised-cosine pulse shaping with rolloff factor of 0.5, it can be seen that PAPR increases significantly for IFDMA whereas PAPR of LFDMA hardly increases. Full comparison of 99.9-percentile PAPR for different modulation formats is in Table I. We can see that IFDMA and LFDMA have lower PAPR than OFDMA consistently.

Fig. 7 shows the impact of rolloff factor  $\alpha$  on the PAPR when using raised cosine pulse shaping, where this impact is more obvious in IFDMA. As the rolloff factor increases from 0 to 1, PAPR reduces significantly for IFDMA. This implies that there is a tradeoff between PAPR performance and out-of-band radiation since out-of-band radiation increases with increasing rolloff factor.

Table 1. Comparison of 99.9-percentile PAPR

Mod. format	IFDMA		LFDMA		OFDMA	
	No pulse shaping	Pulse shaping (rolloff 0.5)	No pulse shaping	Pulse shaping (rolloff 0.22)	No pulse shaping	Pulse shaping (rolloff 0.22)
QPSK	0 dB	4.3 dB	6.1 dB	7.5 dB	7.6 dB	7.6 dB
8PSK	0 dB	4.2 dB	5.9 dB	7.4 dB	7.5 dB	7.5 dB
16QAM	3.5 dB	6.6 dB	7.7 dB	8.4 dB	8.4 dB	8.5 dB
32QAM	3.4 dB	6.4 dB	7.5 dB	8.2 dB	8.3 dB	8.4 dB
64QAM	4.8 dB	7.1 dB	8.0 dB	8.6 dB	8.7 dB	8.7 dB

#### IV. CONCLUSION

In this paper, we analyze the PAPR of SC-FDMA signals and compare it with the case of OFDMA. Specifically, we derive the time domain signals of IFDMA and LFDMA, and numerically compare PAPR characteristics using CCDF of PAPR. It is shown that SC-FDMA signals indeed have lower PAPR compared OFDMA. Also, we have shown that LFDMA incurs higher PAPR compared to IFDMA, but compared to OFDMA, it is lower, though not significantly. Another noticeable fact is that pulse shaping increases PAPR and that rolloff factor in the case of raised-cosine pulse shaping has a significant impact on PAPR of IFDMA. A pulse shaping filter should be designed carefully in order to reduce the PAPR without degrading the system performance.

In conclusion, to fully exploit the low PAPR advantage of SC-FDMA, IFDMA is more desirable than LFDMA when choosing subcarrier mapping method.

#### REFERENCES

- [1] L. J. Cimini, Jr., "Analysis and Simulation of a Digital Mobile Channel Using Orthogonal Frequency Division Multiplexing," *IEEE Trans. Commun.*, vol. 33, no. 7, July 1985, pp. 665–675.
- [2] H. Sari, G. Karam and I. Jeanclaude, "An Analysis of Orthogonal Frequency-Division Multiplexing for Mobile Radio Applications", *Proc. IEEE VTC '94*, pp. 1635–1639, Stockholm, Sweden, June 1994.
- [3] H. Sari, G. Karam and I. Jeanclaude, "Frequency-Domain Equalization of Mobile Radio and Terrestrial Broadcast Channels," *Proc. IEEE GLOBECOM '94*, pp. 1–5, San Francisco, CA, Nov. 1994.
- [4] D. Falconer, S. L. Ariyavisitakul, A. Benyamin-Seeyar and B. Eidson, "Frequency Domain Equalization for Single-Carrier Broadband Wireless Systems," *IEEE Commun. Mag.*, vol. 40, no. 4, April 2002, pp. 58–66.
- [5] 3rd Generation Partnership Project (3GPP); Technical Specification Group Radio Access Network; Physical Layer Aspects for Evolved UTRA, <http://www.3gpp.org/ftp/Specs/html-info/25814.htm>
- [6] U. Sorger, I. De Broeck and M. Schnell, "Interleaved FDMA - A New Spread-Spectrum Multiple-Access Scheme," *Proc. IEEE ICC '98*, pp. 1013–1017, Atlanta, GA, June 1998.
- [7] T. S. Rappaport, *Wireless Communications: Principles and Practice*, Second Edition. Prentice Hall, 2002
- [8] S. H. Han and J. H. Lee, "An Overview of Peak-to-Average Power Ratio Reduction Techniques for Multicarrier Transmission," *IEEE Wireless Commun.*, vol. 12, no. 2, April 2005, pp. 56–65.